Foehnlike Wind with a Traditional Foehn Effect plus Dry-Diabatic Heating from the Ground Surface Contributing to High Temperatures at the End of a Leeward Area

YUYA TAKANE,[a] HIROAKI KONDO,[a,b] HIROYUKI KUSAKA,[c] JIN KATAGI,[d,h] OSAMU NAGAFUCHI,[e,f] KOYOMI NAKAZAWA,[e,f] NAOKI KANEYASU,[a] AND YOSHIHIRO MIYAKAMI[g]

[a] *Environmental Management Research Institute, National Institute of Advanced Industrial Science and Technology, Tsukuba, Japan*
[b] *Japan Weather Association, Tokyo, Japan*
[c] *Center for Computational Sciences, University of Tsukuba, Tsukuba, Japan*
[d] *College of Agro-biological Resource Sciences, University of Tsukuba, Tsukuba, Japan*
[e] *Kyushu University Museum, Kyushu University, Fukuoka, Japan*
[f] *Comprehensive Research Organizations of Fukuoka Institute of Technology, Fukuoka, Japan*
[g] *Environmental Division, Tajimi City Government, Tajimi, Japan*

(Manuscript received 20 July 2016, in final form 27 March 2017)

ABSTRACT

A foehn wind is an important factor in the occurrence of many extreme high-temperature events in geographically complex regions. In this study, the authors verified the hypothesis that a foehnlike wind contributes to high temperatures at the end of the leeward (eastward) area using three difference approaches: field experiments, numerical experiments, and statistical analyses. According to the hypothesis, a foehnlike wind has the features of the sum of a traditional foehn effect with adiabatic heating, plus dry-diabatic heating from the ground surface along the fetch of the wind. Field experiments conducted at seven observational points on Nobi Plain, Japan, where a mesoscale westerly wind blew, revealed that the westerly wind clearly had the features of a traditional foehn effect in the western part of the Nobi Plain. In addition to field experiments, a simplified estimate using a simple mixed-layer model demonstrated that the wind was further heated by dry-diabatic heating (sensible heat supply) from the ground surface along the fetch (especially in urbanized areas in the eastern region of the Nobi Plain) of the wind. This diabatic heating effect along the fetch of the wind on the high temperature at the end of the leeward area was also supported by both additional numerical experiments and a statistical analysis. These results proved that the hypothesis is correct and indicated that ground conditions and the land use and land cover in the windward area were strongly related to air temperature at the end of the leeward area, where an extremely high temperature was observed.

1. Introduction

Extreme high-temperature (EHT) events, including heat waves relating to climate change, have recently occurred frequently in many parts in the world (e.g., IPCC 2013), such as the European heat wave in the summer of 2003 and the EHTs of over 50°C observed in India during June 2016.

EHT events are triggered not only by global and synoptic factors (e.g., Schär et al. 2004; Chase et al. 2006; Black et al. 2004; Fink et al. 2004), but also by meso- and microscale factors. With regard to mesoscale factors, EHT events in geographically simple regions, such as an urban area on a large flat region, can be induced by the urban heat island (UHI) effect (e.g., Grossman-Clarke et al. 2010; Li and Bou-Zeid 2013). However, in geographically complex regions, including near complex terrain, basins, seas, and urban areas, EHTs are influenced by many factors, such as UHI, foehn winds, basin effects (including thermally induced local circulations, e.g., valley wind), and sea breezes (e.g., Takane et al. 2017). A foehn wind is one of the dominant factors in the occurrence of many EHT events in geographically complex regions (Takane and Kusaka 2011; Takane et al. 2013, 2014, 2015; Mori and Sato 2014; Chen and Lu 2016). For example, Takane et al. (2013) indicated that airflow over a mountain with the foehn effect contributed to high-temperature events occurring in the Osaka–Kyoto region when synoptic-scale wind flowed

[h] Current affiliation: Graduate School of Life and Environmental Sciences, University of Tsukuba, Tsukuba, Japan.

Corresponding author: Yuya Takane, takane.yuya@aist.go.jp.

DOI: 10.1175/JAMC-D-16-0257.1

© 2017 American Meteorological Society. For information regarding reuse of this content and general copyright information, consult the AMS Copyright Policy (www.ametsoc.org/PUBSReuseLicenses).

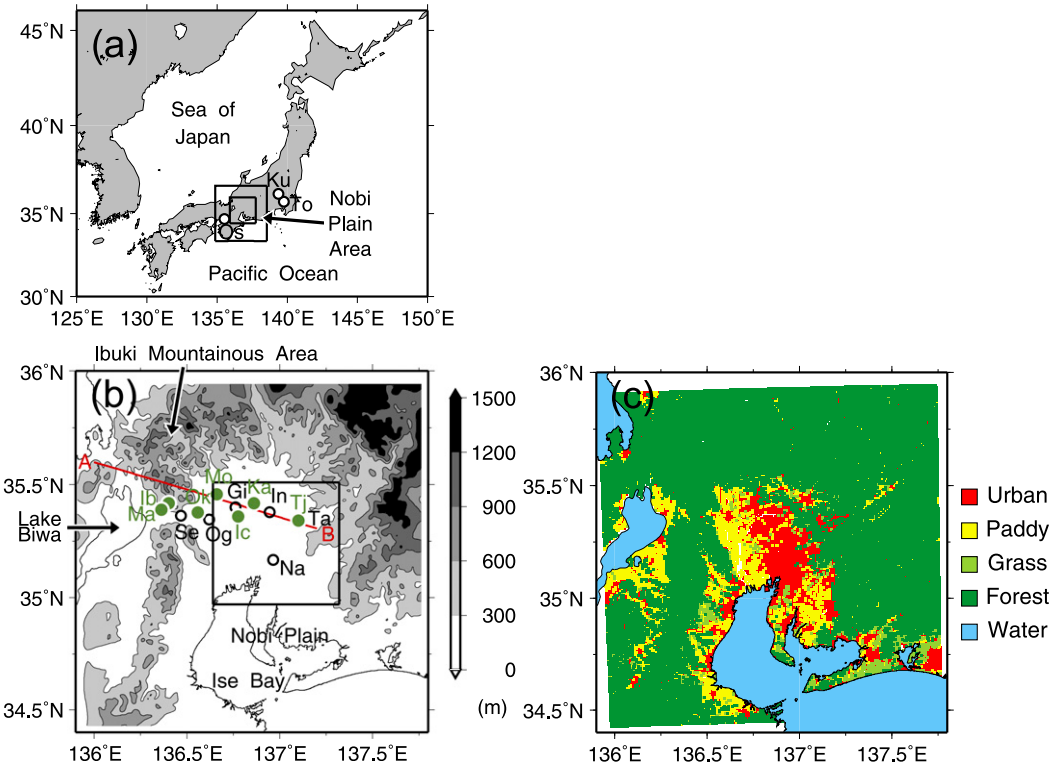

FIG. 1. (a) Map of Japan with the outline of the Nobi Plain area with site locations: Kumagaya (Ku), Tokyo (To), and Osaka (Os). Outer and inner squares indicate domains 1 and 2 of the numerical simulation, respectively. (b) The topography and (c) land-use categories in the Nobi Plain area with site locations of the AMeDAS sites used in the study (black circles): Tajimi (Ta), Nagoya (Na), Gifu (Gi), Ogaki (Og), Inuyama (In), and Sekigahara (Se), and our own field experiment sites (green circles): Ibuki Mt. (Ib), Maibara (Ma), Ogaki (Ok), Motosu (Mo), Ichinomiya (Ic), Kakamigahara (Ka), and Tajimi (Tj). The square in (b) indicates domain 3 of the numerical simulation. The red line A–B is used in Fig. 8.

from a southeast mountainous area. Mori and Sato (2014) showed that foehn winds were a dominant factor in May of high-temperature events occurring in the Okhotsk (Hokkaido) area of Japan. Therefore, understanding the mechanisms of foehn winds that cause EHTs is important for predicting EHT events in geographically complex regions.

Generally, foehn winds can be categorized into types I (a thermodynamic foehn: Hann 1866, 1867) and II (a dynamic foehn: Hann 1866; von Ficker 1920; Seibert 1990) depending on the mechanism of temperature increases in the leeward area. In this study, we refer to these two types as traditional foehns. Recently, the mechanisms of both types have been quantitatively analyzed by the Lagrangian heat budget approach using high-resolution numerical models (Takane and Kusaka 2011; Takane et al. 2015; Miltenberger et al. 2016).

Takane and Kusaka (2011) investigated a record-breaking EHT event of 40.9°C in Kumagaya in the northern part of the Tokyo metropolitan area and revealed that a foehnlike wind (Fig. 16 in Takane and Kusaka 2011) was the dominant factor. This foehnlike wind is similar to type II except that the temperature is more greatly increased by diabatic heating with subgrid-scale turbulent diffusion and sensible heat flux from the ground (Takane and Kusaka 2011; Takane et al. 2015). In other words, the foehnlike wind has the features of a sum of the traditional dry foehn effect with adiabatic heating plus dry-diabatic heating (sensible heat flux) from the ground surface over the fetch of the wind. This wind was also reported by Ishizaki and Takayabu (2009) and Mori and Sato (2014). In the Kumagaya case, the airflow passed through the mixed layer developed on the Chubu Mountains and flowed into the inland region of the Tokyo metropolitan area (Takane et al. 2015). Dry-diabatic heating is more dominant when dry ground conditions occur because of continually clear skies. The foehnlike wind is key to this study and will be referred to below.

Takane et al. (2017) showed that a westerly–northwesterly mesoscale wind frequently blows to the inland area of the Nobi Plain, Japan (Fig. 1), when high temperatures are observed around Tajimi, Gifu Prefecture, which is located at the northeast end of the Nobi Plain. They suggested that this mesoscale wind corresponds

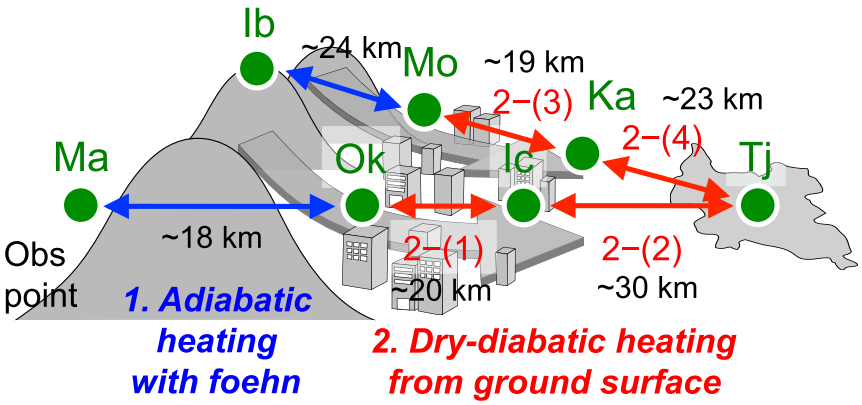

FIG. 2. A concept diagram of the field experiment and analysis undertaken in this study. Green circles indicate our own field experiment sites: Ib, Ma, Ok, Mo, Ic, Ka, and Tj. Black numbers indicate approximate distances between sites.

to a foehnlike wind, which contributes to the EHT events in the city. This hypothesis, proposed by Takane et al. (2017), suggests that ground conditions and land use and land cover (LULC) in the windward area of Tajimi are likely to be strongly related to air temperature at Tajimi, which is the end of the leeward area. However, their hypothesis has not been verified by any previous studies. Such a study would be important to assess the impact of LULC change associated with urban planning and development on the air temperature in Tajimi and other leeward areas.

In this study, we attempted to verify the hypothesis that a foehnlike wind with adiabatic and dry-diabatic heating from the ground surface contributed to the high temperatures at the end of the leeward area, initially through a field experiment (sections 3a and 3b). The hypothesis was also verified by numerical experiments (section 3c) and a statistical analysis (section 3d) from the perspective of soil moisture, which controls the amount of dry-diabatic heating (sensible heat flux) from the ground surface.

2. Data and methodology

a. Field experiment and data collection

We conducted field experiments at seven points around the Nobi Plain from 1 to 31 August 2015 to observe surface meteorological elements in the locations at which the mesoscale westerly wind blew over the Nobi Plain. The Maibara (Ma), Ogaki (Ok), Ichinomiya (Ic), and Tajimi (Tj) stations were located along the track of the mesoscale westerly wind (route W; Figs. 1 and 2). In addition, the Motosu (Mo), Kakamigahara (Ka), and Tajimi (Tj) stations were located along the track of the mesoscale northwesterly wind (route NW; Figs. 1 and 2). There are two reasons for the selection of the two routes used in this study: 1) because of a previous study (Takane et al. 2012, 2017) and to test numerical simulations conducted by the authors that showed that the mesoscale winds frequently blew along these two routes and 2) to cross-check the result for one route by using the results for another route. The remaining station, Ibuki Mt., was located at the top of Mount Ibuki (height about 1340 m). Therefore, data collected at this station were used to analyze the traditional foehn wind and estimate the mixed-layer height. All stations were located in fallow fields (same LULC), with open space.

A multiweather sensor (WXT520; Vaisala, Vantaa, Finland) was used to measure air temperature (°C), relative humidity (%), horizontal wind components ($m\,s^{-1}$), air pressure (hPa), and precipitation (mm) at 2.0 m above ground level. A pyranometer (PCM-01NB-L10; Prede Co., Tokyo, Japan) and soil moisture meter (WD-3-L5, ThetaProbe ML3-L5; Delat-T Devices Ltd., Burwell, United Kingdom) were used to record solar radiation ($W\,m^{-2}$) at ground level and volume water content (%) at 10 cm below ground level, respectively. In this study, potential temperatures were estimated by using air temperature and air pressure. The recording interval was set to 1 s, and average values were recorded over 1 min (60 samples) and used for analysis.

Here, we explain the principles of the field experiment and subsequent analysis. In route W, we considered whether the mesoscale westerly wind had the features of a traditional foehn effect using potential temperature and wind data observed at Ogaki (a relatively leeward point) and Maibara (a relatively windward point) (Fig. 2). If the potential temperature and wind speed observed at Ogaki were higher than those at Maibara under a westerly wind condition, we concluded that this westerly wind had the features of a traditional foehn. This judgment was based on the general definition of a

foehn wind. Moreover, we diagnosed the onset of the foehn phenomenon based on a vertical cross section of potential temperature, water vapor, horizontal and vertical wind velocities, and the Froude number as calculated by a numerical model (section 3c). No vertical observations over the Nobi Plain area were available to determine whether or not a foehn had occurred. Therefore, we relied on the simulation results. Additionally, dry-diabatic heating from the ground surface over the fetch of the wind was estimated by the potential temperature difference between Ogaki and Ichinomiya [2–(1); Fig. 2] and Ichinomiya and Tajimi [2–(2); Fig. 2]. A similar analysis to that for route W was also conducted for route NW. Specifically, we considered whether the mesoscale northwesterly wind had the feature of a traditional foehn effect, using potential temperature and wind data observed at Motosu (a relatively leeward point) and Ibuki Mt. (a windward mountain point) (Fig. 2), and using numerical simulation results. The dry-diabatic heating from the ground surface over the fetch of the wind was also estimated by the potential temperature difference between Motosu and Kakamigahara [2–(3); Fig. 2], and Kakamigahara and Tajimi [2–(4); Fig. 2].

In this study, we used surface weather charts [fax chart(s) SPAS and ASAS from the Japan Meteorological Agency (JMA)] recorded at 0900 Japan standard time (JST: UTC + 9 h), automated meteorological data acquisition system (AMeDAS) data provided by the JMA, and soil water index (SWI) data (Okada et al. 2001), in addition data to obtained from the field experiment. The SWI is an indicator of the amount of water in the soil, and can be used to represent the risk of sediment-related disasters (http://www.jma.go.jp/jma/en/News/2011_soil_water_index.html); it is represented as a grid point value with 5-km and 3-h horizontal and temporal resolutions. These SWI data were used in the analyses discussed in sections 3b and 3c.

b. Numerical experiment

We used the Weather Research and Forecasting (WRF) Model, version 3.1.1 (Skamarock et al. 2008), to determine dry-diabatic heating from the windward ground surface in section 3c. This version of the WRF Model has a good track record for reproducing EHT events and local wind in geographically complex regions (e.g., Takane et al. 2015). The model domains were d01, d02, and d03 (Fig. 1), consisting of 120 × 130, 181 × 181, and 199 × 199 grid points in the x and y directions, respectively. We set the horizontal grid spacing to 2.7, 0.9, and 0.3 km in domains 1, 2, and 3, respectively. The model top was 50 hPa with 42 vertical sigma levels. The initial and boundary conditions used in this simulation were basically the same as in the work on Takane et al. (2015), but the National Centers for Environmental Prediction–National Center for Atmospheric Research (NCEP–NCAR) reanalysis data (Kalnay et al. 1996) were used as land surface data. In this simulation, soil moisture data from the NCEP–NCAR reanalysis, with a 1° horizontal resolution, were corrected using the relationship between SWI data with a 5-km horizontal resolution and the observed volume water content (Fig. 3a). Time integration was conducted continuously from 1200 UTC 9 to 12 August 2015.

As in the work of Takane and Kusaka (2011) and Takane et al. (2015), the LULC and topographic datasets of the Geospatial Information Authority of Japan (GIAJ) were used. We used the same parameterizations as used by Takane and Kusaka (2011) (Table 1).

3. Results and discussion

a. Field experiment

During the observation period, there were 8 days with clear-sky conditions (i.e., the duration of sunshine at the Tajimi AMeDAS site was longer than 6 h without precipitation; Takane et al. 2017) and a westerly–northwesterly wind was blowing over the Nobi Plain. In this study, we considered the results on 11 August 2015 as typical, with clear-sky conditions and a westerly–northwesterly wind. The horizontal distribution of surface air temperature and wind observed by AMeDAS at 1500 JST 11 August 2015 around the Nobi Plain is shown in Fig. 4, which indicates that a westerly–northwesterly mesoscale wind was blowing across the Nobi Plain. This mesoscale wind kept blowing from morning until sunset (not shown). This wind system frequently occurs when high temperatures are observed at Tajimi (Takane et al. 2017).

Figure 5a shows diurnal variations of surface potential temperature observed at the points along the route W and Ibuki Mt. In this study, a westerly–northwesterly wind is defined as when the wind direction at each point was >225° and <337.5°. This figure shows that a westerly–northwesterly wind blew continuously from 0600 JST to the evening at all points, except for Tajimi. This westerly–northwesterly wind reached Tajimi around 1000 JST from the western part of the Nobi Plain.

Here, we discuss whether the westerly wind has the features of a traditional foehn using the potential temperature and wind data observed at Ogaki and Maibara, as mentioned in section 2 (Fig. 2). Figure 5a shows that the potential temperature observed at Ogaki was higher than that observed at Maibara. In addition, the wind speed observed at Ogaki was continuously 1.1 m s^{-1} higher than that observed at Maibara (not shown). These results suggest that the differences in potential temperature and wind speed between the two points

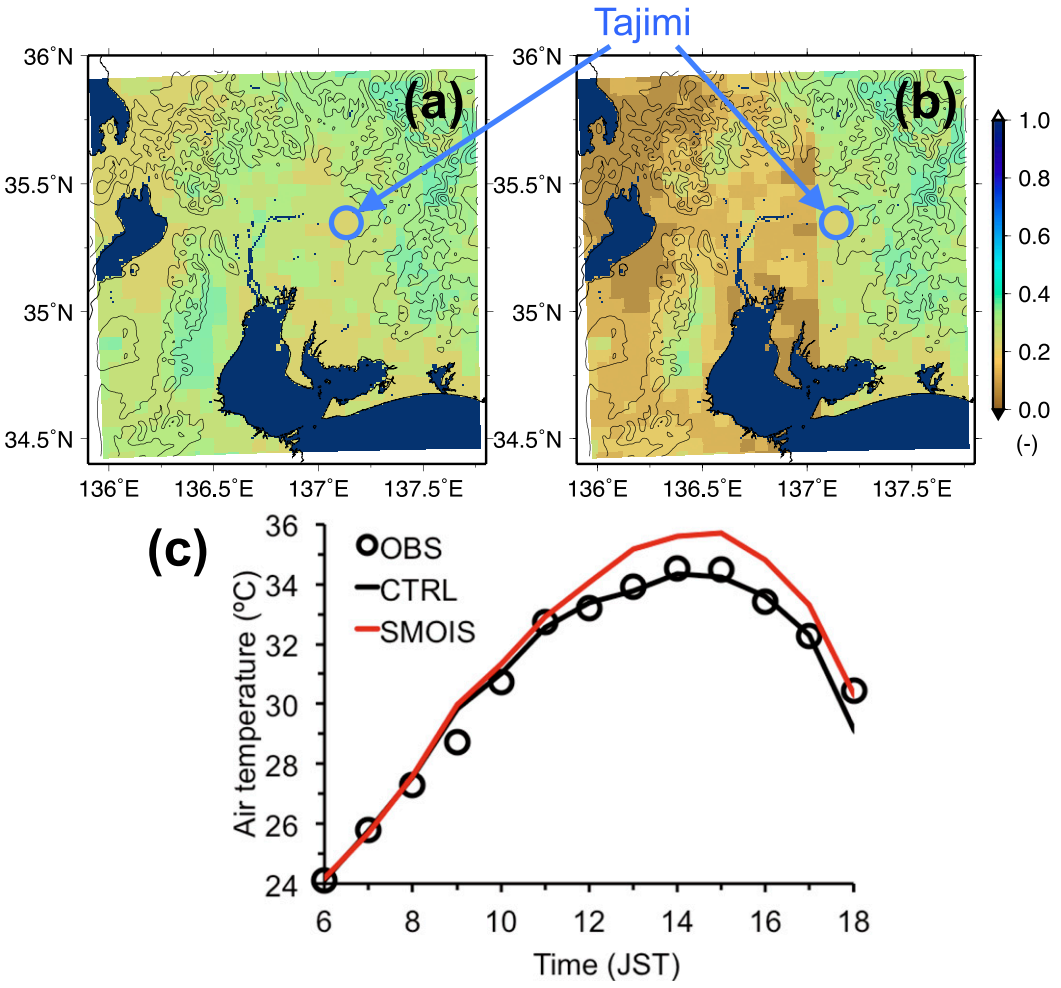

FIG. 3. Horizontal distributions of the initial conditions of soil moisture for (a) CTRL and (b) SMOIS. (c) Diurnal variations in the surface air temperature observed at Tajimi (circles), simulated by the CTRL (black solid line), and SMOIS (red solid line) on 11 Aug 2015.

were caused by a traditional foehn effect, with a downslope wind that originated from above the windward area around Maibara to around the Ogaki observational point (ground level) through the col. This local downslope wind has been reported by previous studies (e.g., Owada 1990; Takane et al. 2017). In general, winds descend easily where a col is present in mountainous areas (e.g., Lilly and Klemp 1979; Smith 1985; Saito 1993). An additional analysis of days with clear-sky conditions and a southerly wind (not a westerly wind) blowing over the Nobi Plain (5, 8, and 9 August 2015) showed the opposite results, with the potential

TABLE 1. Physics of the WRF Model used in this study (Takane and Kusaka 2011).

	Physics	Reference
Microphysics	WRF single-moment 3-class (WSM3)	Hong et al. (2004); Dudhia (1989)
Radiation (longwave)	Rapid Radiative Transfer Model (RRTM)	Mlawer et al. (1997)
Radiation (shortwave)	Dudhia	Dudhia (1989)
Boundary layer	Mellor–Yamada–Janjić (MYJ)	Mellor and Yamada (1982); Janjić (2002)
Surface layer	MYJ (based on similarity theory; Monin and Obukhov 1954)	Janjić (1996, 2002)
Land surface (no urban area)	Noah land surface model (LSM)	Chen and Dudhia (2001)
Land surface (urban area)	Single-layer urban canopy model (UCM)	Kusaka et al. (2001); Kusaka and Kimura (2004a,b)

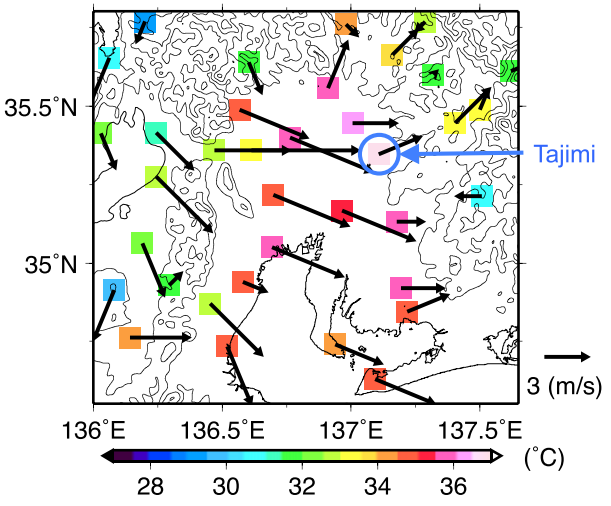

FIG. 4. Horizontal distributions of surface air temperature (colored squares) and wind (vectors) observed by AMeDAS sites at 1500 JST 11 Aug 2015. Black solid lines indicate elevation with 300-m contour intervals.

temperature and wind speed observed at Ogaki being lower than those observed at Maibara (not shown). These results support the conclusion that the relatively high potential temperature and wind speed observed at Ogaki on 11 August 2015 were caused by a traditional foehn effect, with a westerly downslope wind. In addition to the above observational evidence, we have additional evidence that a traditional foehn occurred during this event; this evidence is shown in section 3c.

Here, we discuss dry-diabatic heating from the ground surface along the fetch of the wind with regard to the potential temperature difference between Ogaki and Ichinomiya [2–(1); Fig. 2)] and between Ichinomiya and Tajimi [2–(2); Fig. 2]. There was a small potential temperature difference between Ogaki and Ichinomiya (Fig. 5a). In contrast, the difference between Ichinomiya and Tajimi was relatively large. Specifically, the potential temperature averaged from 1000 to 1400 JST at Tajimi was 1.8°C higher than that at Ichinomiya. The difference can be seen from early morning to evening and became large after 1000 JST, when a westerly wind began to blow at Tajimi. This result suggests that the relatively large potential temperature difference after 1000 JST was caused by the advection of air parcels heated from the ground surface in the area leeward of the col. The accumulated solar radiation from sunrise to 1400 JST at Tajimi was 17.8 MJ m^{-2}, which was smaller than the 18.7 MJ m^{-2} at Ichinomiya. This suggests that the heat input due to advection contributed to the temperature rise at Tajimi, because the surface air temperature at Tajimi should have been low compared to that at Ichinomiya if only solar radiation had contributed one-dimensionally to air temperature through the surface heat budget process.

As described above, the potential temperature difference between Ogaki and Ichinomiya was small, but the difference between Ichinomiya and Tajimi was relatively large. There is a possibility that this difference was due to the difference of the diabatic heating from the surface under different LULCs. The LULC around the western part of the Nobi Plain (between Ogaki and Ichinomiya) roughly corresponds to paddy fields and grassland (Fig. 1c). The sensible heat supplied from

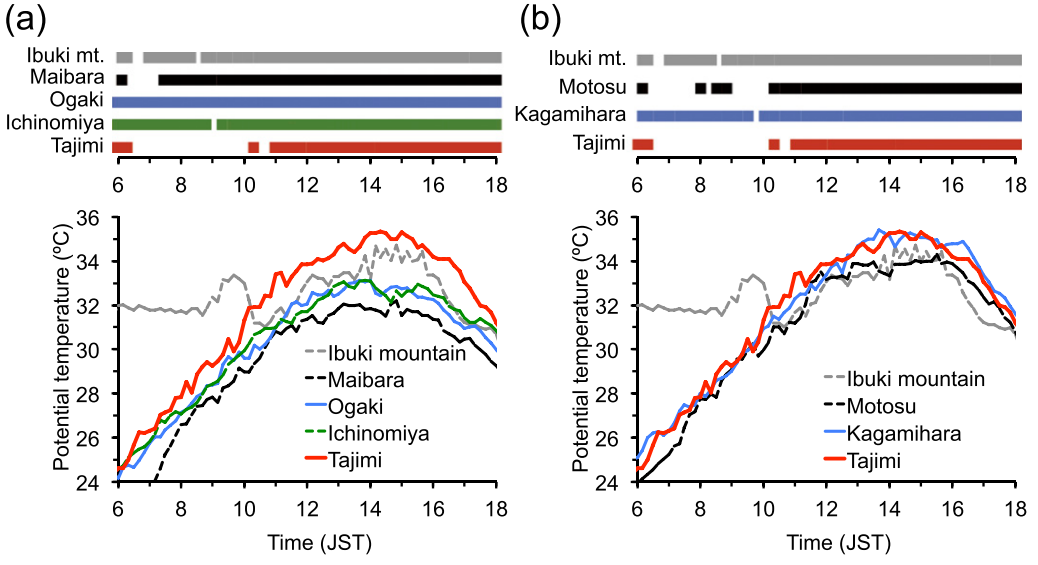

FIG. 5. Diurnal variations in the northwest–westerly wind, with a wind direction larger than 225° and smaller than 337.5° (bars), and potential temperature (lines) observed along (a) route W and (b) route NW on 11 Aug 2015.

these ground surfaces to the westerly wind is relatively small. As a result, the potential temperature at Ichinomiya tended to increase only slightly compared to the potential temperature increase at Ogaki. In contrast, the LULC around the eastern part of the Nobi Plain (between Ichinomiya and Tajimi) is urban, except for a small basin located west of Tajimi city (Fig. 1c). Therefore, the sensible heat supplied from the ground surface to the westerly wind is relatively large, which contributed to the potential temperature increase at Tajimi compared to Ichinomiya.

b. *Diabatic heating derived using a mixed-layer model*

To confirm this, the simplified estimate of the effect of diabatic heating from the ground surface (especially from an urban surface) on the potential temperature increase on the leeward area was obtained using a simple mixed-layer model (Kimura 1994), and the results were compared to the observed potential temperatures. Specifically, we considered a situation where an atmospheric column moves over an inhomogeneous ground surface from the windward to the leeward direction by mesoscale winds during daytime, when the westerly wind penetrates in Tajimi (Fig. 6). In this situation, the mean potential temperature of an atmospheric column increased $\Delta\theta$(°C) when this column moved from the windward to the leeward direction because of the difference in the sensible heat flux (ΔH; W m^{-2}) from the inhomogeneous ground surface along the fetch of the wind (Fig. 6). In this model, ΔH is defined as a value that depends on only the difference of LULC (urban or nonurban), which means that we did not consider time changes of sensible heat flux over urban or nonurban surfaces (Fig. 6). This assumption is reasonable for the purpose of a simple estimate as described above. We estimated this $\Delta\theta$ and compared it to the observed potential temperature differences. Here, we assumed that the sensible heat flux at the leeward point H_{lee} was ΔH higher than that at the windward point H_{wind} (i.e., $\Delta H = H_{\text{lee}} - H_{\text{wind}}$). The length of the fetch is L (m), and wind speed is U (m s^{-1}). An accumulated sensible heat supply from the fetch to an atmospheric column ΔQ (J m^{-2}) can be described as

$$\Delta Q = \Delta H L/U. \tag{1}$$

The sensible heat supply ΔQ (J m^{-2}) needed to increase the $\Delta\theta$ of an atmospheric column when the mixed-layer height is h(m) is

$$\Delta Q = C_p \rho \Delta\theta h. \tag{2}$$

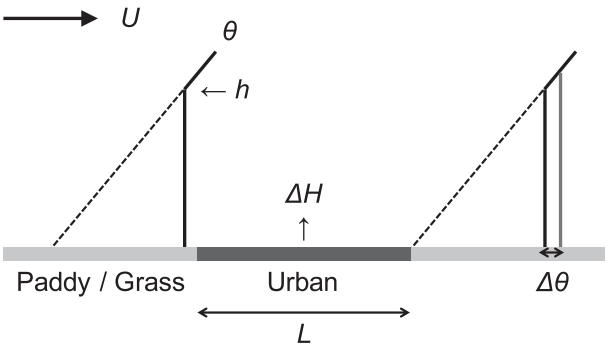

FIG. 6. Schematic representation of simple mixed-layer model. This figure is a modification of Fig. 12.14 in Kimura (1994).

When (1) and (2) are the same, the mean potential temperature increase of the atmospheric column can be described as

$$\Delta\theta = \Delta H[L/(C_p \rho h U)]. \tag{3}$$

Here, C_p is the specific heat of air (J kg^{-1} K^{-1}) and ρ is the density of dry air (kg m^{-3}). The value of h was estimated as follows. The diurnal variation of the vertical profile of potential temperature was estimated using the potential temperatures observed at six observational points on the Nobi Plain and one point at Mount Ibuki (1340-m height). This estimate showed that daytime potential temperature averaged for the six points located in the Nobi Plain was higher than at Mount Ibuki (not shown), which suggests that h reached at least 1340 m in this event. In addition, a pilot balloon observation conducted at Inuyama (Fig. 1) on 21 August 2011, when weather conditions were similar to 11 August 2015, showed that h reached at least 1000 m. Therefore, h was set at 1340 m for this estimate. The L between Tajimi and Ichinomiya was 30 km, and that between Ichinomiya and Ogaki was 20 km (Fig. 2). The U were set at 2.9 and 4.9 m s^{-1} based on observational results at Ichinomiya and Ogaki (average values for the period of 1000–1400 JST), respectively. Then, ΔH was determined based on the results of a numerical simulation conducted in section 3b. This numerical simulation showed that the daily average sensible heat at the windward point (H_{wind}), corresponding to a paddy–grassland cover, was 33.5 W m^{-2} on 11 August 2015. The daily average sensible heat at the leeward point (H_{lee}), corresponding to urban land cover, was 192.2 W m^{-2}. The daily averaged sensible heat flux in August 2001 in Tokyo (Kugahara) observed by Moriwaki and Kanda (2004) was about 180 W m^{-2}, which is consistent with the simulated value for the urban grid given above. In this analysis, the ΔH was set at 158.7 W m^{-2} between Tajimi and Inuyama, because the LULC around the eastern part of the Nobi

Plain (between Ichinomiya and Tajimi) corresponded to urban land cover, except for a small basin located west of Tajimi city. The ΔH was set at $0.0\,\mathrm{W\,m^{-2}}$ between Inuyama and Ogaki, because the LULC around the western part of the Nobi Plain (between Ogaki and Ichinomiya) roughly corresponded to paddy field and grassland, which is a similar LULC as in the more windward area (horizontally homogeneous LULC condition).

The simple estimate using the equations and parameters described above showed that the $\Delta\theta$ between Tajimi and Ichinomiya was 1.1°C during daytime, which is consistent with the observational results of 1.8°C described above. Because ΔH was set to $0.0\,\mathrm{W\,m^{-2}}$, as described above, the $\Delta\theta$ between Ichinomiya and Ogaki was 0.0°C, which was also consistent with the observational results of 0.2°C. These were simple estimates because ΔH was constant with time and advection and diffusion processes (such as entrainment) at the top and sides of the atmospheric column could not be considered. However, the results suggest that the observed potential temperature differences between two points were roughly caused by diabatic heating from the ground surface over the fetch of the wind. The results also showed that the amount of diabatic heating was dependent on LULC.

To check the consistency of route W's results, we considered whether the northwesterly wind along route NW had the features of a traditional foehn wind, with diabatic heating from the ground surface as was apparent with the westerly wind along route W. First, a traditional foehn wind with airflow over the mountain was considered in terms of the potential temperature and wind data observed at Motosu and Ibuki Mt., as mentioned in section 2 (Fig. 2). This is a common method to confirm the foehn effect with airflow over the mountain (e.g., Plavcan et al. 2014). Figure 5b shows that potential temperatures observed at Motosu and Ibuki Mt. were similar after 1000 JST when the northwesterly wind began to blow at Motosu. This result suggests that air parcels were transported by the northwesterly downslope wind from a point near Ibuki Mt. to near the ground surface around Motosu. In addition, the wind speed observed at Motosu was similar to that at Ibuki Mt. after about 1000 JST (not shown). This result suggests that momentum was transported from near the height of Ibuki Mt. to near the ground surface around Motosu, which also supports the occurrence of a traditional foehn wind along route NW. An additional analysis of days with a clear sky and southerly wind blowing over the Nobi Plain (5, 8, and 9 August 2015) showed that daytime potential temperatures observed at Ibuki Mt. were over 3°C higher than that of Motosu (not shown). This result supports the conclusions drawn above. A numerical simulation (section 3c) also supports these conclusions.

Next, we considered the dry-diabatic heating from the ground surface over the fetch of the northwesterly wind using the potential temperature difference between Motosu and Kakamigahara [2–(3)], and Kakamigahara and Tajimi [2–(4), Fig. 2]. Potential temperatures observed at Kakamigahara and Tajimi, which are located in the leeward area compared to Motosu, were 0.7°C (average value for 1000–1400 JST) higher than at Motosu. The same pattern was found for surface air temperature. The accumulated solar radiation from sunrise to 1400 JST at Motosu was $18.9\,\mathrm{MJ\,m^{-2}}$, which was larger than the $18.0\,\mathrm{MJ\,m^{-2}}$ value at Kakamigahara and $17.8\,\mathrm{MJ\,m^{-2}}$ at Tajimi. This suggests that heat input due to advection contributed to the air temperatures at Ichinomiya and Tajimi, because the surface air temperature at Kakamigahara and Tajimi tended to become small compared to that of Motosu if only solar radiation contributed one-dimensionally to air temperature through the surface heat budget. Figure 5b shows that the potential temperature difference between Motosu and Kakamigahara was large, but the difference between Kakamigahara and Tajimi was relatively small. It is possible that this difference was caused by the difference in the sensible heat flux (diabatic heating) from the different LULC, as in route W. The LULC between Motosu and Kakamigahara roughly corresponded to urban area, including Gifu city, the capital of the prefecture (Fig. 1c). The amount of sensible heat supplied from the ground surface to the northwesterly wind was relatively large. As a result, sensible heat from the ground surface to the northwesterly wind was relatively large, which contributed to the potential temperature increase at Kakamigahara compared to Motosu. In contrast, the LULC between Kakamigahara and Tajimi corresponded to forest or grass (Fig. 1c). Therefore, the potential temperature at Tajimi tended to increase only slightly compared to that of Kakamigahara.

We also estimated the $\Delta\theta$ along route NW using the simple mixed-layer model and compared it to the observed potential temperature differences. The simple estimate showed that $\Delta\theta$ between Motosu and Kakamigahara was 0.7°C, which was consistent with the observational result described above.

The results of the field experiment clearly showed that the westerly and northwesterly winds had the features of a traditional foehn wind. In addition, these winds were also influenced by dry-diabatic heating from the ground surface over the fetch of the wind, which was suggested by the observational results of potential temperature differences between leeward and windward points, and a simple estimate using a simple mixed-layer model. A schematic representation of the foehnlike wind, with adiabatic and dry-diabatic heating from the ground

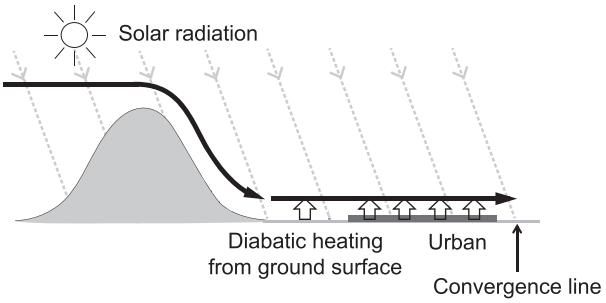

FIG. 7. Schematic representation of a foehnlike wind, which has the features of the sum of a traditional foehn effect with adiabatic heating, plus dry-diabatic heating from the ground surface over the fetch of the wind.

surface, is shown in Fig. 7. To verify the effect of the dry-diabatic heating from the ground surface over the fetch of the wind on the temperature increase in the leeward area by different approaches, a numerical experiment and a statistical analysis were conducted and the results are described in sections 3b and 3c, respectively.

c. *Numerical experiment*

The diurnal variation of surface air temperature at Tajimi simulated by the control (CTRL) as described in section 2b is shown in Fig. 3c, which indicates that the CTRL satisfactorily reproduced the diurnal variation of observed air temperature. The CTRL also reproduced the horizontal distributions of surface air temperature and wind speed over the Nobi Plain (not shown). In general, the WRF Model can reproduce the diurnal variations and horizontal distributions of the summertime air temperature and wind in the Japanese plains, which has been reported by previous studies (e.g., Takane et al. 2012, 2013, 2015). The model setting of this study was based on the studies mentioned above.

Figure 8 shows the vertical cross section of the potential temperature along line A–B in Fig. 1b for the CTRL case, which suggests that the onset of traditional foehn occurred in this event for the following reasons: 1) Potential temperature differences cannot be seen near the surface between windward (136.00°–136.25°) and leeward (136.60°–farther eastward) at 0800 JST but can be seen after 1200 JST. 2) the Froude numbers [Fr = $U/(N/h)$; U: mean wind speed, N: Brunt–Väisälä frequency, and h: mountain height] calculated where windward area are approximately 1.0 (depending on time and location), which means that mountain airflow has the potential to cross the mountain, and the downslope wind is appropriately simulated (not shown). 3) Cloud and precipitation were not calculated and observed in the windward area, meaning that air parcels were not heated diabatically by water vapor

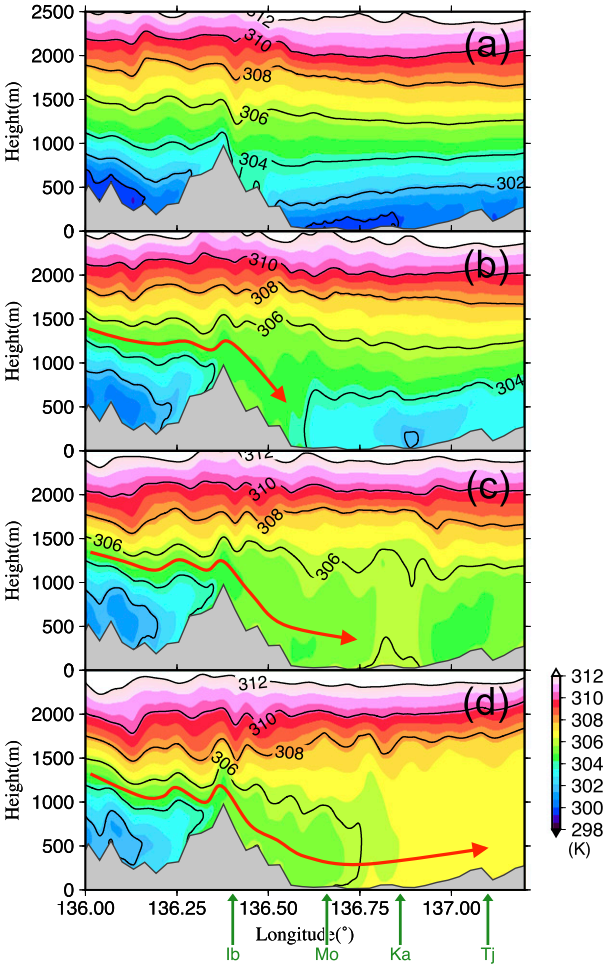

FIG. 8. Vertical cross section of the potential temperature (shading and contours) on 11 Aug 2015: (a) 0800, (b) 1000, (c) 1200, and (d) 1400 JST along line A–B in Fig. 1b for the CTRL case. The red lines show diagnostic airflow of the downslope wind.

condensation; they essentially flowed along the isentrope. For these reasons, we can state that air parcels between 1300 and 1500 m over the windward area in the morning moved eastward and then crossed the mountaintop approximately at 0800 JST (Fig. 8a). The parcels then descended along the mountain slope and reached the near surface near Motosu at 1000 JST (Fig. 8b). The parcels passed Motosu after 1000 JST (Fig. 8c) and then crossed an isentrope as a result of diabatic heating from the ground surface and reached Kakamigahara and Tajimi (Fig. 8d). The results of the numerical simulation support our assessment of the onset of traditional foehn using surface observational data as described in section 2a.

Figure 9a shows the diurnal variation of the surface heat budget at Ichinomiya point, which had a windward location compared to Tajimi when the westerly wind blew over the Nobi Plain. In this simulation, the maximum sensible heat flux at Ichinomiya was about

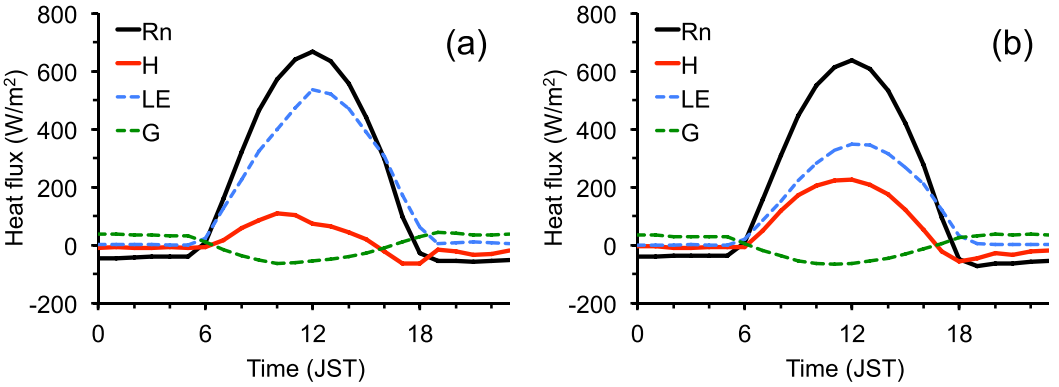

FIG. 9. Surface heat budgets simulated by (a) the CTRL and (b) SMOIS on 11 Aug 2015 at Ichinomiya. Black solid lines indicate net radiation R_n; red solid lines indicate sensible heat flux H; blue dashed lines indicate latent heat flux LE; green dashed lines indicate ground heat flux G.

100 W m^{-2}, which was lower than the maximum latent heat flux of about 500 W m^{-2}. A similar feature was also simulated at Motosu and Tajimi.

The sensitivity of the surface air temperature in the leeward area of Tajimi to sensible heat flux over the windward area (Fig. 9b) of the westerly–northwesterly wind was numerically examined to verify the effects of dry-diabatic heating from the ground surface over the fetch of the wind. In this experiment, we reduced the soil moisture by 15% from the initial condition of the CTRL in the windward area (Figs. 3a,b). Other model conditions were unchanged. This experiment was referred to as the sensitivity experiment of soil moisture (SMOIS). In general, the amount of dry-diabatic heating from the ground surface (sensible heat flux) depends on the soil moisture when sunshine input is constant. The surface heat budget (Bowen ratio) can easily be modified in this experiment by simply modifying the soil moisture in the model. This experiment is physically reasonable compared to an experiment that changes only one component of the surface heat budget (e.g., sensible heat flux) in the model. The effectiveness of this experiment was reported by Takane and Kusaka (2011). The results of the SMOIS showed that the surface energy budget (Bowen ratio) at Ichinomiya changed from the CTRL to SMOIS. Specifically, the maximum latent heat flux decreased to about 150 W m^{-2} (became about 350 W m^{-2}) from about 500 W m^{-2} in the CTRL. In contrast, the maximum sensible heat flux increased to about 100 W m^{-2} from about 100 W m^{-2} in the CTRL. The surface heat budget at Tajimi was almost unchanged from the CTRL to SMOIS. Figure 3c indicates that surface air temperatures at Tajimi simulated by the CTRL and SMOIS were almost the same before about 1100 JST, but the temperature simulated by SMOIS was clearly higher than that of the CTRL after around 1100 JST when the westerly wind began to blow at Tajimi in the experiments. This result demonstrated that the surface air temperature increased at Tajimi via the advection of the westerly wind heated from the ground surface over the windward area, and supports the results of the field experiment described in section 3a.

d. *Statistical analysis*

The effect of diabatic heating from the ground surface on air temperature in the leeward area was also assessed by a statistical analysis using observational data taken from the JMA, and SWI data. The analysis period was July–August 2010–15, which was a period in which SWI data were available. Days with clear skies, with a sunshine duration of more than 6 h and without precipitation, were selected from the analysis period. Over the 372 days in the analysis period, 170 were clear-sky days. Note that the diurnal variation of the SWI during August 2015 (including the response to precipitation) corresponded basically to that of the actual soil moisture data observed by the authors (not shown). Therefore, it is reasonable to use SWI data as an index of soil moisture data. In this analysis, we defined the westerly wind days based on surface wind direction and speed observed at Ogaki and Tajimi, and the horizontal distribution of the surface wind system observed by AMeDAS over the Nobi Plain. There were 56 westerly wind days in this period, which are a subset of the 170 clear-sky days.

The relationship between the SWI averaged for several points located in the western area of Tajimi and the surface air temperature at 1400 JST observed at the Tajimi AMeDAS on clear-sky days is shown in Fig. 10. This figure shows that the air temperature at 1400 JST on Tajimi was negatively correlated with the SWI in the western area of Tajimi. The correlation coefficient was -0.37^{**}. Single and double asterisks indicate 5% and 1% levels of statistical significance, respectively. The

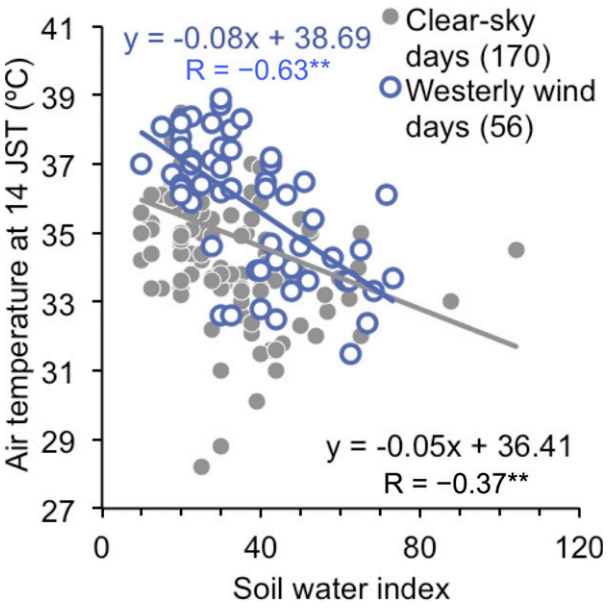

FIG. 10. Scatter diagram of the SWI averaged over several points in the western area of Tajimi vs the surface air temperature at 1400 JST observed at the Tajimi AMeDAS from July to August 2010–15. The gray and blue circles indicate clear-sky and westerly wind days, respectively.

negative correlation suggests that dry ground conditions cause an increase in the sensible heat flux from the ground surface, which contributes one-dimensionally to an air temperature increase directly above the ground at not only the western area of Tajimi, but also in Tajimi city. The surface air temperature averaged for clear-sky days at 1400 JST on Tajimi was 34.9°C.

Note that the relationship between the SWI and air temperature on westerly wind days (-0.63^{**}) was stronger than that on clear-sky days (-0.37^{**}). The difference between these correlation coefficients was statistically significant at the 5% level. The surface air temperature averaged for westerly wind days at 1400 JST on Tajimi was 35.8°C, which was about 1°C higher than the clear-sky day temperature of 34.9°C. These results suggest that the air temperature at Tajimi increased not only because of the local sensible heat supply from the dry ground surface but also because of the advective sensible heat supply with the advection of the westerly wind heated from the windward ground surface over the fetch of the wind.

Additional statistical analysis showed that the air temperature at Tajimi tended to be higher with an increase in solar radiation. This feature was stronger on westerly wind days than on clear-sky days. In general, a relatively large solar radiation, with dry ground conditions and a westerly wind blowing, contributed to an increase in the sensible heat flux from the ground surface. These results indicated that the air temperature at Tajimi tended to be high when a relatively larger sensible heat flux was supplied from the windward ground surface to the westerly wind. The results of the statistical analyses supported the results of the field and numerical experiments described above. Conversely, there was no correlation between air temperature at Tajimi and daytime wind speed, which is related to the fetch time during which dry-diabatic heating can occur. This suggests that soil moisture and sunshine over the windward area have a more important role than the wind speed to air temperature at Tajimi.

e. Comparison of the Tajimi and Kumagaya cases

Takane and Kusaka (2011) indicated that a sensible heat supply from the mountain surface (windward area) enhanced the foehn effect and contributed to the EHT of 40.9°C in Kumagaya (leeward area), as mentioned in the introduction. In general, the sensible heat flux in mountainous areas is larger than that of a flat plain when the LULC is exactly the same (Kimura 1994). The sensible heat supply from the mountain surface was the main factor in the generation of the foehnlike wind above Kumagaya. In contrast, the sensible heat supply from the flat plain, especially in the urban area, was important for the occurrence of the foehnlike wind at Tajimi (Fig. 7). The results of this study suggest that the surface air temperature in the leeward area will increase more if urbanization continues in the windward area in the near future, and if dry ground conditions, including on the mountain surface, become more prevalent.

4. Summary

In this study, we verified the hypothesis that a foehnlike wind contributes to the high temperatures at the end of the leeward area using three different approaches: field experiments, numerical experiments, and a statistical analysis. According to the hypothesis, the foehnlike wind has the features of the sum of a traditional foehn effect with adiabatic heating plus dry-diabatic heating from the ground surface over the fetch of the wind.

Field experiments conducted at seven observational points along the track of the mesoscale westerly–northwesterly wind that blew over the Nobi Plain revealed the westerly–northwesterly wind clearly had the features of a traditional foehn effect at the western part of the Nobi Plain. Specifically for route W, the surface potential temperature and wind speed observed at the leeward point of Ogaki were higher those at the windward point of Maibara because of the westerly downslope wind that originated from above the windward area around Maibara to around Ogaki (ground level). In route NW, the surface potential temperature and wind speed observed at the leeward point of Motosu were roughly

similar to the values observed at the windward mountain point of Ibuki Mt. because of the northwesterly downslope wind from near Ibuki Mt. to near the ground surface around Motosu. These results are typical features of a traditional foehn effect with downslope wind and were not observed on nonwesterly wind days (southerly wind days).

The field experiments indicated that the wind also had the features of dry-diabatic heating from the ground surface over the fetch of the wind because the potential temperature observed at the leeward point of Tajimi was clearly higher than at the windward points. A simplified estimate, produced by a simple mixed-layer model, suggested that the potential temperature differences between the leeward and windward points were mainly caused by a sensible heat supply (diabatic heating) from the dominant LULC of the ground surface over the fetch of the wind. To cross-check the effect of dry-diabatic heating from the ground surface over the fetch of the wind on the temperature increase at the end of the leeward area, a numerical experiment and a statistical analysis were conducted.

The sensitivity of surface air temperature at the end of the leeward area (Tajimi) to soil moisture over the windward area of the westerly–northwesterly wind was numerically examined using the WRF Model. The results showed that surface air temperatures at Tajimi simulated by the CTRL and SMOIS were almost the same before about 1100 JST, but the temperature simulated by SMOIS was clearly higher than that simulated by the CTRL after about 1100 JST when the westerly wind began to blow at Tajimi in the experiments. This result indicated that surface air temperature increased at Tajimi because of advection of the westerly wind through heat supplied from the ground surface over the windward area, thereby supporting the results of the field experiments.

The effect of diabatic heating from the ground surface on air temperature in the leeward area was also assessed by a statistical analysis. The results showed that the daytime air temperature at Tajimi was negatively correlated to the SWI in the western area of Tajimi. The relationship between SWI and air temperature on westerly wind days was higher than on clear-sky days. These results statistically suggest that the air temperature at Tajimi increased not only because of the one-dimensional sensible heat supply from the dry ground surface but also because of the two-dimensional sensible heat supply with the advection of the westerly wind heated from the windward ground surface over the fetch of the wind. Additional analysis indicated that the air temperature at Tajimi tended to be high when a relatively large sensible heat flux was released from the windward ground surface to the westerly wind. The statistical analyses supported the results of the field and numerical experiments.

It is important to note that the effect of the diabatic heating over the fetch of the wind on the high temperature in the leeward area was supported not only by field experiments, but also by numerical experiments and statistical analysis. These results prove that the hypothesis is correct and indicate that ground conditions and the LULC in the windward area were strongly related to air temperature at the end of the leeward area. The results of this study will contribute to progress in the study of foehn effects and provide new knowledge regarding the effect of LULC changes, including urban planning and development, in the windward region on the changes in air temperature in the leeward area.

Acknowledgments. We thank two anonymous reviewers for providing valuable comments that helped us to improve the manuscript. This research was performed under a Partnership Agreement between the Center for Computational Sciences, University of Tsukuba, and Tajimi city. We thank Dr. Shigeki Hirose, Mr. Junji Hibino, Mr. Kazumi Furuta, Mr. Akira Furuta, Mr. Kironobu Iinuma, Mr. Haruki Murase, Mr. Hidekazu Nagasawa, Mr. Yoshikazu Nakai, Mrs. Harumi Okamura, and Prof. Yukihiro Kikegawa of Meisei University, who helped with observations in several cities in the Chubu area during August 2015. This study was supported by JSPS KAKENHI Grant-in-Aid for Young Scientists (A) Number 26702006. The numerical simulations were performed under the Interdisciplinary Computational Science Program in the Center for Computational Sciences, University of Tsukuba. The free software package Generic Mapping Tools (GMT) was used to draw the figures.

REFERENCES

Black, E., M. Blackburn, G. Harrison, B. Hoskins, and J. Methven, 2004: Factors contributing to the summer 2003 European heatwave. *Weather*, **59**, 217–223, doi:10.1256/wea.74.04.

Chase, T. N., K. Wolter Sr., R. A. Pielke, and I. Rasool, 2006: Was the 2003 European summer heat wave unusual in global context? *Geophys. Res. Lett.*, **33**, L23709, doi:10.1029/2006GL027470.

Chen, F., and J. Dudhia, 2001: Coupling an advanced land surface–hydrology model with the Penn State–NCAR MM5 modeling system. Part I: Model description and implementation. *Mon. Wea. Rev.*, **129**, 569–585, doi:10.1175/1520-0493(2001)129<0569:CAALSH>2.0.CO;2.

Chen, R., and R. Lu, 2016: Role of large-scale circulation and terrain in causing extreme heat in western north China. *J. Climate*, **29**, 2511–2527, doi:10.1175/JCLI-D-15-0254.1.

Dudhia, J., 1989: Numerical study of convection observed during the winter monsoon experiment using a mesoscale two-dimensional model. *J. Atmos. Sci.*, **46**, 3077–3107, doi:10.1175/1520-0469(1989)046<3077:NSOCOD>2.0.CO;2.

Fink, A. H., T. Brücher, A. Krüger, G. C. Leckebusch, J. G. Pinto, and U. Ulbrich, 2004: Factors contributing to the summer 2003 European heatwave. *Weather*, **59**, 209–216, doi:10.1256/wea.73.04.

Grossman-Clarke, S., J. A. Zehnder, T. Loridan, and S. B. Grimmond, 2010: Contribution of land use changes to near-surface air temperatures during recent summer extreme heat events in the Phoenix metropolitan area. *J. Appl. Meteor. Climatol.*, **49**, 1649–1664, doi:10.1175/2010JAMC2362.1.

Hann, J., 1866: Zur Frage über den Ursprung des Föhn (The question of the origin of the foehn). *Z. Österr. Ges. Meteor.*, **1**, 257–263.

——, 1867: Der Föhn in den österreichischen Alpen (The foehn in the Austrian Alps). *Z. Österr. Ges. Meteor.*, **2**, 433–445.

Hong, S.-Y., J. Dudhia, and S.-H. Chen, 2004: A revised approach to ice microphysical processes for the bulk parameterization of clouds and precipitation. *Mon. Wea. Rev.*, **132**, 103–120, doi:10.1175/1520-0493(2004)132<0103:ARATIM>2.0.CO;2.

IPCC, 2013: Summary for policymakers. *Climate Change 2013: The Physical Science Basis*, T. F. Stocker et al., Eds., Cambridge University Press, 1–29.

Ishizaki, N., and I. Takayabu, 2009: On the warming events over Toyama Plain by using NHRCM. *SOLA*, **5**, 129–132, doi:10.2151/sola.2009-033.

Janjić, Z. I., 1996: The surface layer in the NCEP Eta Model. Preprints, *11th Conf. on Numerical Weather Prediction*, Norfolk, VA, Amer. Meteor. Soc., 354–355.

——, 2002: Nonsingular implementation of the Mellor–Yamada level 2.5 scheme in the NCEP Meso model. NCEP Office Note, 436, 61 pp.

Kalnay, E., and Coauthors, 1996: The NCEP/NCAR 40-Year Reanalysis Project. *Bull. Amer. Meteor. Soc.*, **77**, 437–471, doi:10.1175/1520-0477(1996)077<0437:TNYRP>2.0.CO;2.

Kimura, F., 1994: Numerical simulation of urban atmosphere (in Japanese). *Meteorology of Water Environment*, Asakura Publishing, 281–307.

Kusaka, H., and F. Kimura, 2004a: Coupling a single-layer urban canopy model with a simple atmospheric model: Impact on urban heat island simulation for an idealized case. *J. Meteor. Soc. Japan*, **82**, 67–80, doi:10.2151/jmsj.82.67.

——, and ——, 2004b: Thermal effects of urban canyon structure on the nocturnal heat island: Numerical experiment using a mesoscale model coupled with an urban canopy model. *J. Appl. Meteor.*, **43**, 1899–1910, doi:10.1175/JAM2169.1.

——, H. Kondo, Y. Kikegawa, and F. Kimura, 2001: A simple single-layer urban canopy model for atmospheric models: Comparison with multi-layer and slab models. *Bound.-Layer Meteor.*, **101**, 329–358, doi:10.1023/A:1019207923078.

Li, D., and E. Bou-Zeid, 2013: Synergistic interactions between urban heat islands and heat waves: The impact in cities is larger than the sum of its parts. *J. Appl. Meteor. Climatol.*, **52**, 2051–2064, doi:10.1175/JAMC-D-13-02.1.

Lilly, D. K., and J. B. Klemp, 1979: The effect of terrain shape on non-linear hydrostatic mountain waves. *J. Fluid Mech.*, **95**, 241–261, doi:10.1017/S0022112079001452.

Mellor, G. C., and T. Yamada, 1982: Development of a turbulence closure model for geophysical fluid problems. *Rev. Geophys. Space Phys.*, **20**, 851–875, doi:10.1029/RG020i004p00851.

Miltenberger, A. K., S. Reynolds, and M. Sprenger, 2016: Revisiting the latent heating contribution to foehn warming: Lagrangian analysis of two foehn events over the Swiss Alps. *Quart. J. Roy. Meteor. Soc.*, **142**, 2194–2204, doi:10.1002/qj.2816.

Mlawer, E. J., S. J. Taubman, P. D. Brown, M. J. Iacono, and S. A. Clough, 1997: Radiative transfer for inhomogeneous atmosphere: RRTM, a validated correlated-k model for the longwave. *J. Geophys. Res.*, **102**, 16 663–16 682, doi:10.1029/97JD00237.

Monin, A. S., and A. M. Obukhov, 1954: Basic laws of turbulent mixing in the surface layer of the atmosphere (in Russian). *Contrib. Geophys. Inst. Acad. Sci., USSR*, **151**, 163–187.

Mori, K., and T. Sato, 2014: Spatio-temporal variation of high-temperature events in Hokkaido, north Japan. *J. Meteor. Soc. Japan*, **92**, 327–346, doi:10.2151/jmsj.2014-404.

Moriwaki, R., and M. Kanda, 2004: Seasonal and diurnal fluxes of radiation, heat, water vapor, and carbon dioxide over a suburban area. *J. Appl. Meteor. Climatol.*, **43**, 1700–1710, doi:10.1175/JAM2153.1.

Okada, K., Y. Makihara, A. Shimpo, K. Nagata, M. Kunitsugu, and K. Saitoh, 2001: Soil water index (SWI) (in Japanese). *Tenki*, **48**, 349–356.

Owada, M., 1990: A climatological study of local winds (oroshi) in central Japan. Doctoral thesis, Institute of Geoscience, University of Tsukuba, 98 pp.

Plavcan, D., G. J. Mayr, and A. Zeileis, 2014: Automatic and probabilistic foehn diagnosis with a statistical mixture model. *J. Appl. Meteor. Climatol.*, **53**, 652–659, doi:10.1175/JAMC-D-13-0267.1.

Saito, K., 1993: A numerical study of the local downslope wind ''Yamaji-kaze'' in Japan. Part 2: Non-linear aspect of the 3-D flow over a mountain range with a col. *J. Meteor. Soc. Japan*, **71**, 247–272, doi:10.2151/jmsj1965.71.2_247.

Schär, C., P. L. Vidale, D. Lüthi, C. Frei, C. Häberli, M. A. Liniger, and C. Appenzeller, 2004: The role of increasing temperature variability in European summer heatwaves. *Nature*, **427**, 332–336, doi:10.1038/nature02300.

Seibert, R. S., 1990: South foehn studies since the ALPEX experiment. *Meteor. Atmos. Phys.*, **43**, 91–103, doi:10.1007/BF01028112.

Skamarock, W. C., and Coauthors, 2008: A description of the Advanced Research WRF version 3. NCAR Tech. Note NCAR/TN-475+STR, 113 pp., doi:10.5065/D68S4MVH.

Smith, R. B., 1985: On severe downslope winds. *J. Atmos. Sci.*, **42**, 2597–2603, doi:10.1175/1520-0469(1985)042<2597:OSDW>2.0.CO;2.

Takane, Y., and H. Kusaka, 2011: Formation mechanisms of the extreme high surface air temperature of 40.9°C observed in the Tokyo metropolitan area: Considerations of dynamic foehn and foehnlike wind. *J. Appl. Meteor. Climatol.*, **50**, 1827–1841, doi:10.1175/JAMC-D-10-05032.1.

——, ——, M. Takaki, M. Okada, S. Abe, T. Nagai, Y. Fuji, and S. Iizuka, 2012: Observational study and numerical prediction experiments on Wet–Bulb Globe Temperature in Tajimi, Gifu prefecture: Consideration of uncertainty with a physical parameterization scheme and horizontal resolution of the Weather Research and Forecasting model (in Japanese with English abstract). *Geogr. Rev. Japan*, **86A**, 14–37.

——, Y. Ohashi, H. Kusaka, Y. Shigeta, and Y. Kikegawa, 2013: Effects of synoptic-scale wind under the typical summer pressure pattern on the mesoscale high-temperature events in the Osaka and Kyoto urban areas by the WRF model. *J. Appl. Meteor. Climatol.*, **52**, 1764–1778, doi:10.1175/JAMC-D-12-0116.1.

——, H. Kusaka, and H. Kondo, 2014: Climatological study on mesoscale extreme high temperature events in inland of the Tokyo metropolitan area, Japan, during the past 22 years. *Int. J. Climatol.*, **34**, 3926–3938, doi:10.1002/joc.3951.

——, ——, and ——, 2015: Investigation of a recent extreme high-temperature event in the Tokyo metropolitan area using numerical simulations: The potential role of a 'hybrid' foehn wind. *Quart. J. Roy. Meteor. Soc.*, **141**, 1857–1869, doi:10.1002/qj.2490.

——, and Coauthors, 2017: Factors causing climatologically high temperature in a hottest city in Japan: A multiscale analysis of Tajimi. *Int. J. Climatol.*, **37**, 1456–1473, doi:10.1002/joc.4790.

von Ficker, H., 1920: Der Einfluss der Alpen auf die Fallgebiete des Luftdruckes und die Entstehung von Depressionen über dem Mittelmeer (The influence of the Alps on the fall of the air pressure and the formation of depression over the Mediterranean). *Meteor. Z.*, **55**, 350–363.